

Electronic Supporting Information for

Formation of all-biopolymer-based composites with cellulose as main component

Alexandra S.M. Wittmar^{a,b}, Oleg Prymak^c, Thomas Homm^d, Felix Surholt^d, Jörg Uhlemann^d, Natalie Stranghöner^d, Mathias Ulbricht^{a,b}

^a*Lehrstuhl für Technische Chemie II, Universität Duisburg-Essen, Universitätsstr. 7, 45141 Essen, Germany.*

^b*NETZ – Nano Energie Technik Zentrum, CENIDE – Center for Nanointegration Duisburg-Essen, Carl-Benz-Str. 199, 47057 Duisburg, Germany.*

^c*Inorganic Chemistry and Center for Nanointegration Duisburg-Essen (CeNIDE), University of Duisburg-Essen, Universitätsstr. 7, 45141 Essen, Germany*

^d*Institut für Metall- und Leichtbau, Universität Duisburg-Essen, Universitätsstr. 15, 45141 Essen, Germany.*

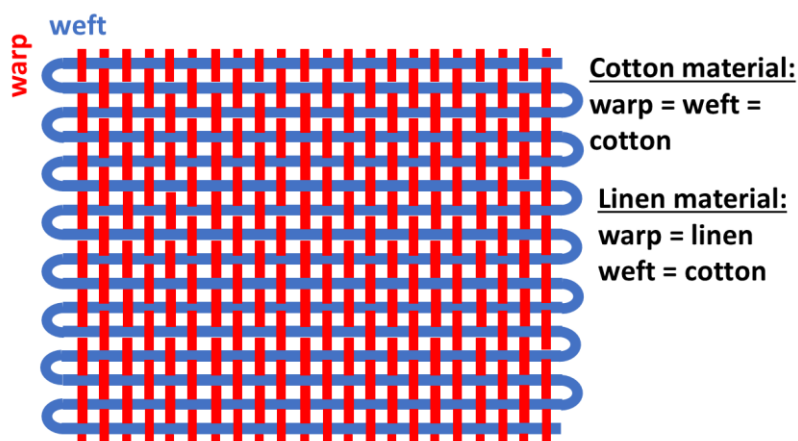


Figure ESI 1. Fiber orientation in the two precursor textile materials

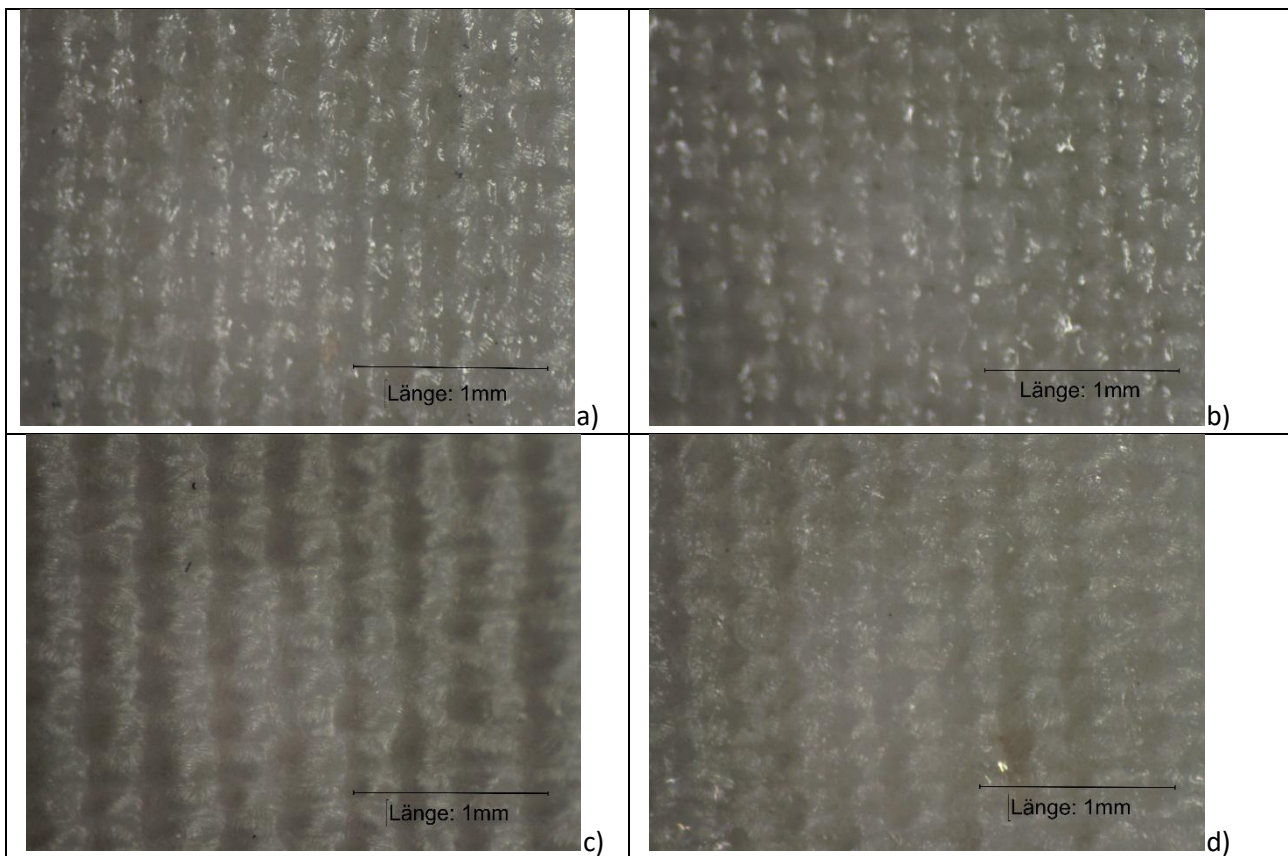


Figure ESI 2. The surface views (LM) for the cotton-based composites prepared in this work:
a)EmimOAc; b) BmimOAC; c) 8% Cellulose and d) 1% Chitosan

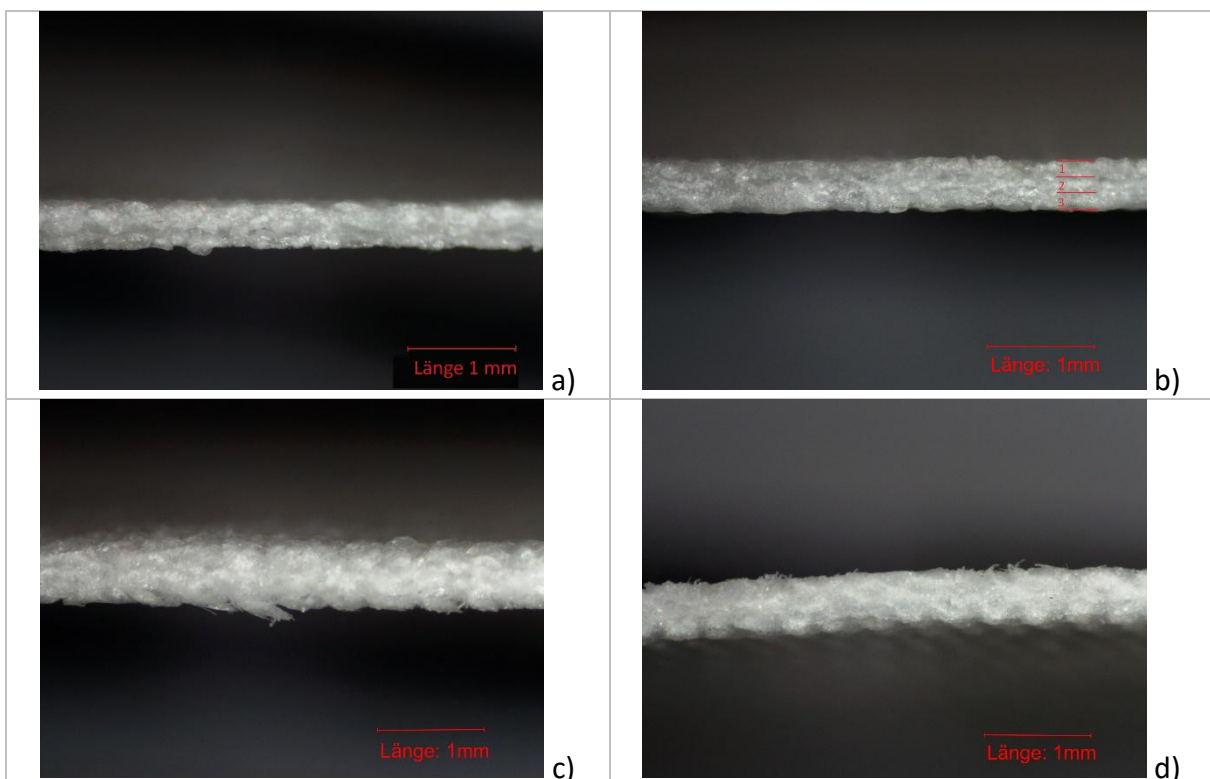


Figure ESI3. The cross-section views (LM) for the cotton-based composites prepared in this work: a)
EmimOAc; b) BmimOAC; c) 8% Cellulose and d) 1% Chitosan

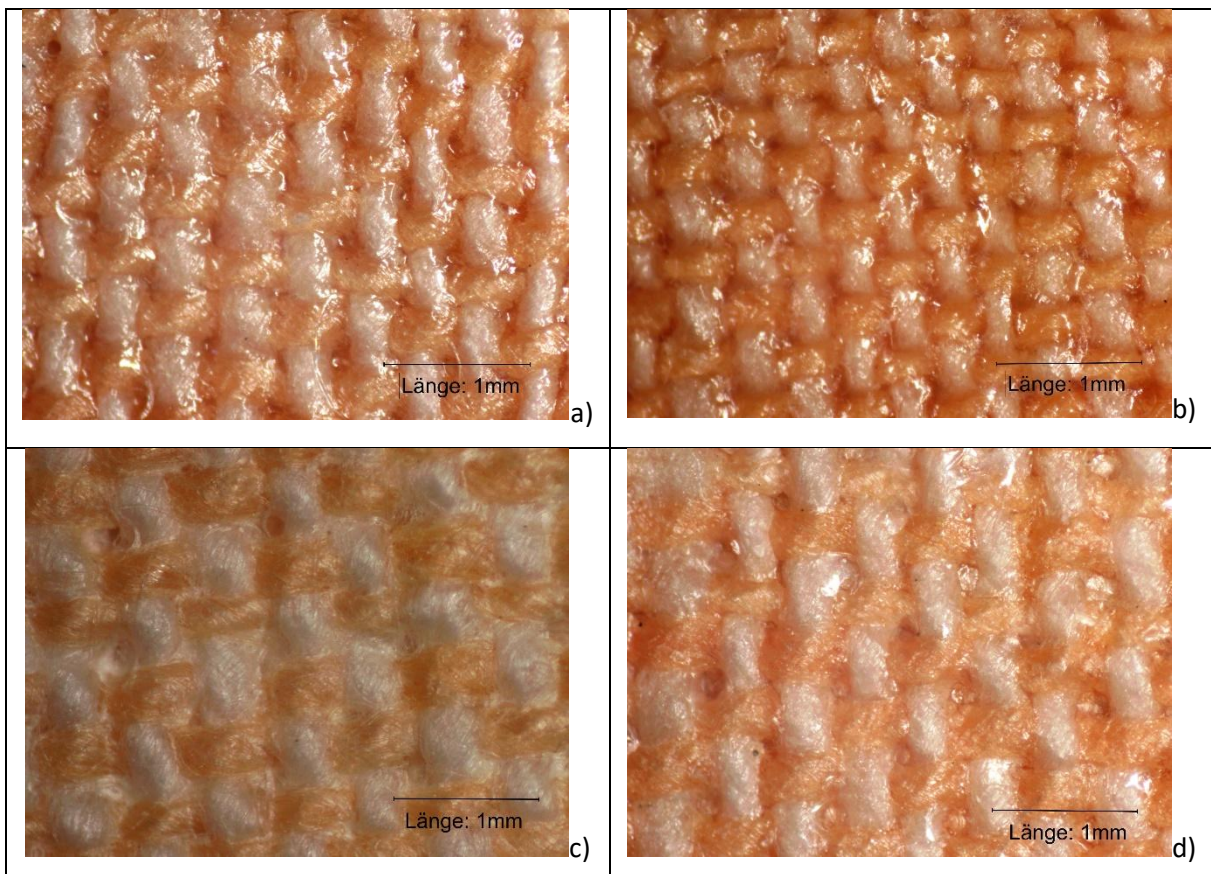


Figure ESI 4. The surface views (LM) for the cotton-based composites prepared in this work:

a)EmimOAc; b) BmimOAC; c) 8% Cellulose and d) 1% Chitosan

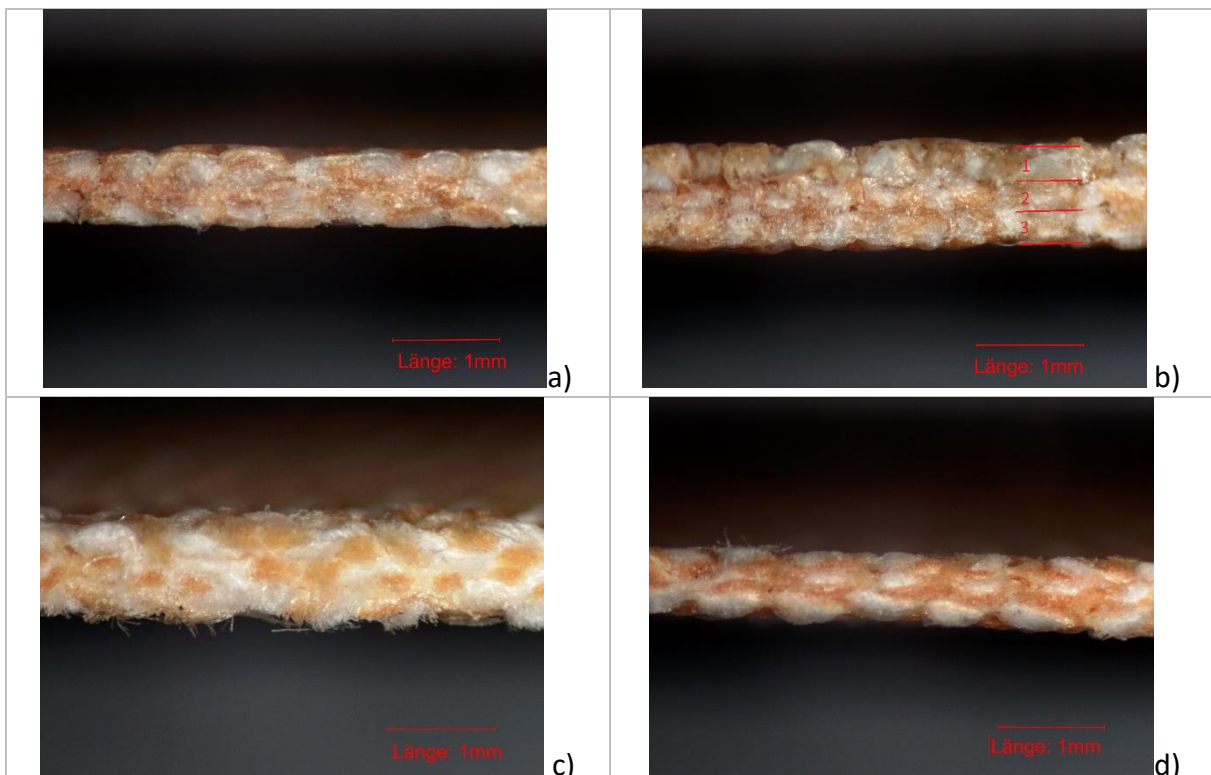


Figure ESI5. The cross-section views (LM) for the linen-based composites prepared in this work:

a) EmimOAc; b) BmimOAC; c) 8% Cellulose and d) 1% Chitosan

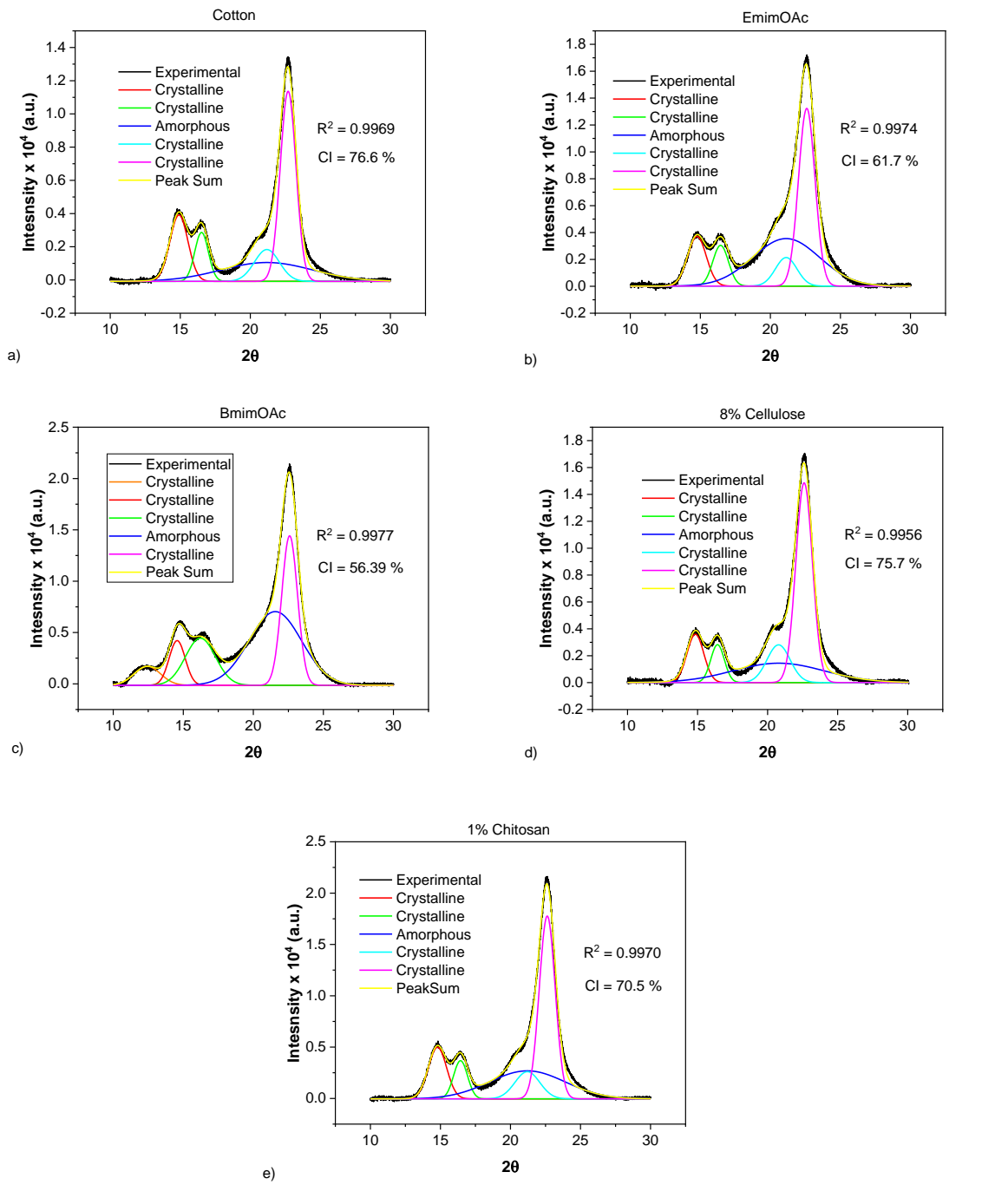


Figure ESI 6. Deconvolution of the XRD patterns for the cellulose in the cotton textile and in the cotton-based composites

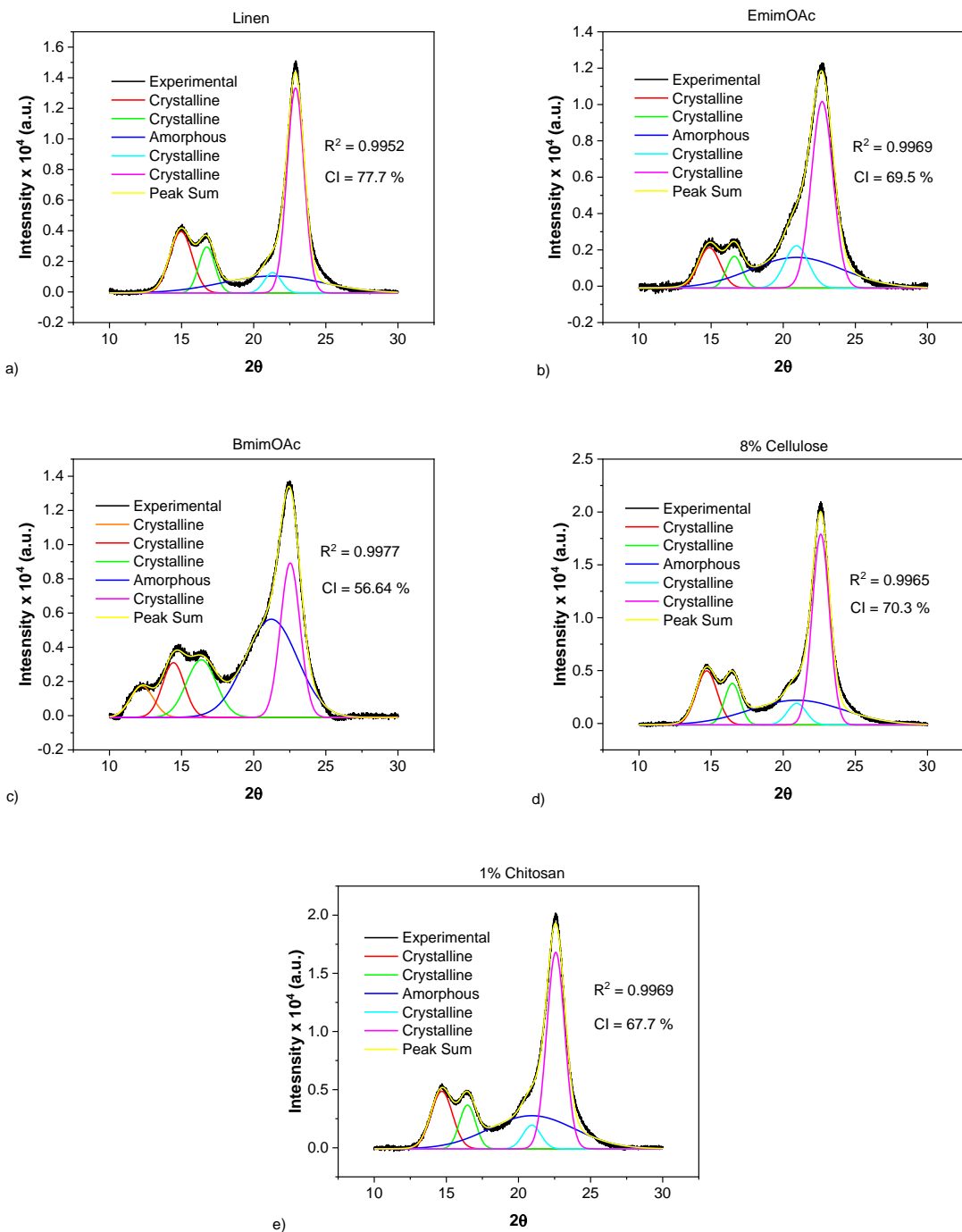


Figure ESI 7. Deconvolution of the XRD patterns for the cellulose in the linen textile and in the linen-based composites

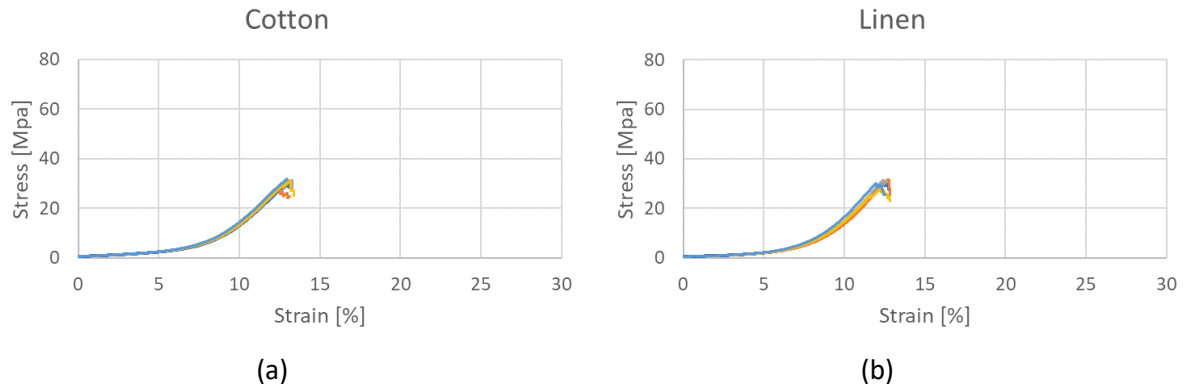


Figure ESI 8. Stress-strain curves for the precursor textile materials: a) cotton and b) linen

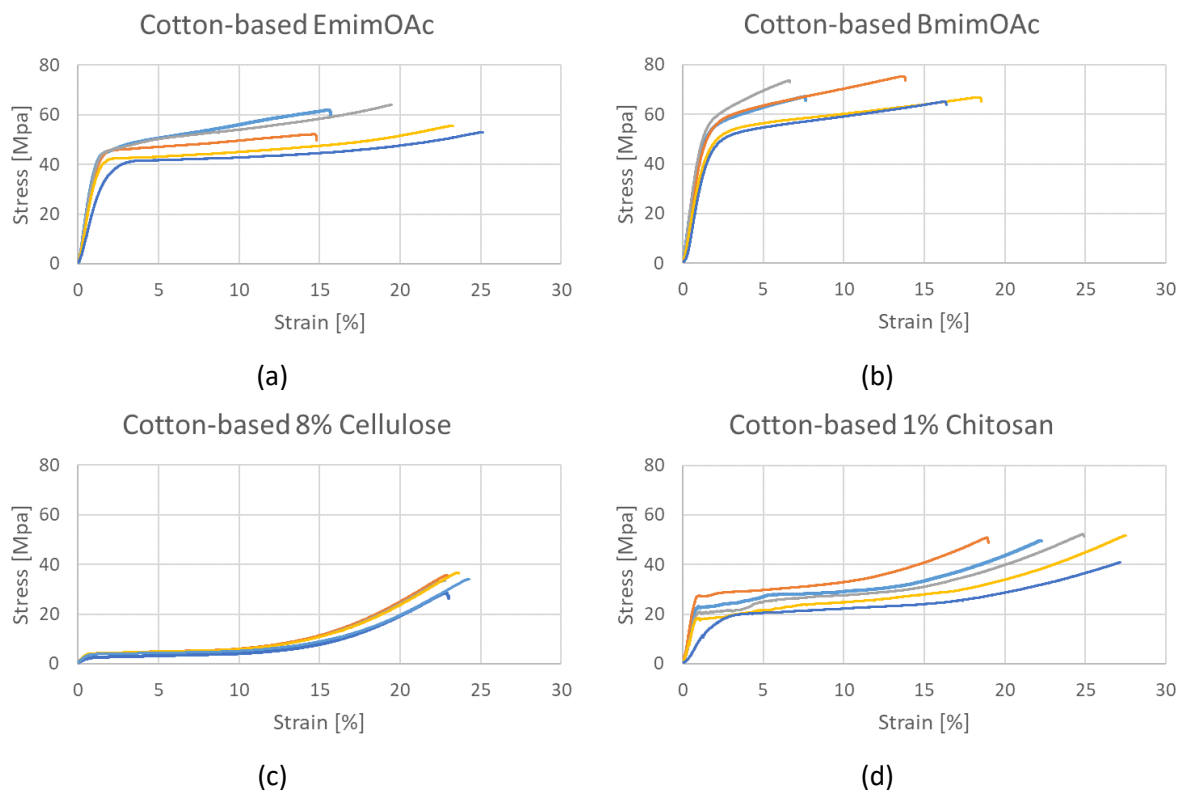


Figure ESI 9. Stress-strain curves for the cotton-based composites: a) EmimOAc; b) BmimOAc; c) 8% Cellulose and d) 1% Chitosan

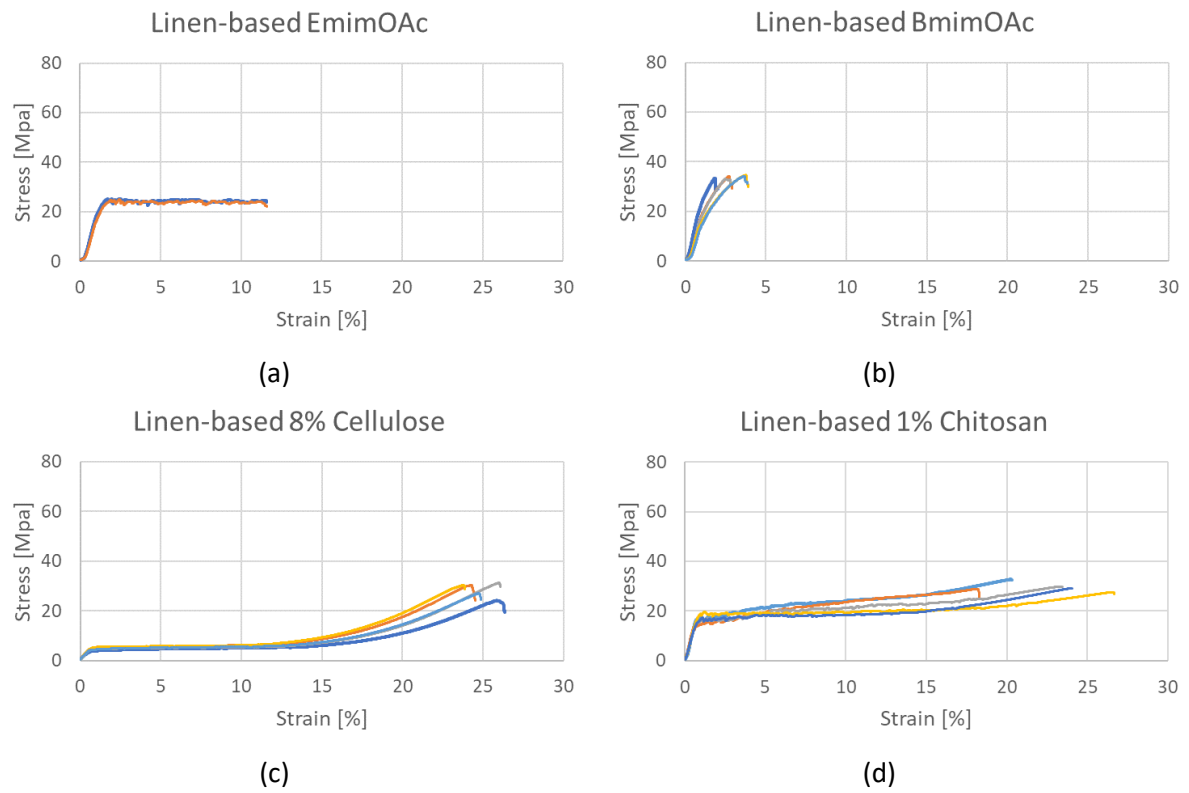


Figure ESI 10. Stress-strain curves for the linen-based composites: a) EmimOAc; b) BmimOAc; c) 8% Cellulose and d) 1% Chitosan

Table ESI1. The obtained composites in the context of other similar materials described in the specialized literature

Sample name	Reinforcement material	Impregnation solution	Processing Temp. [°C]	Density [g/cm³]	Crystallinity index [%]	Tensile strength [MPa]	Reference
EmimOAc (C)	cotton textile	EmimOAc	80 °C	1.15	~ 62 %	~57	this work
BmimOAc (C)	cotton textile	BmimOAc	80 °C	1.40	~ 56 %	~ 70	this work
8% Cellulose (C)	cotton textile	8% Cellulose in EmimOAc:DMSO= 30:70	80 °C	0.70	~ 76 %	~34	this work
1% Chitosan (C)	cotton textile	1% Chitosan in EmimOAc:DMSO= 50:50	80 °C	1.04	~ 71 %	~ 49	this work
EmimOAc (L)	linen textile	EmimOAc	80 °C	1.11	~ 70 %	~ 25	this work
BmimOAc (L)	linen textile	BmimOAc	80 °C	1.02	~ 57 %	~ 34	this work
8% Cellulose (L)	linen textile	8% Cellulose in EmimOAc:DMSO= 30:70	80 °C	0.65	~ 70 %	~ 29	this work
1% Chitosan (L)	linen textile	1% Chitosan in EmimOAc:DMSO= 50:50	80 °C	0.96	~ 68 %	~ 30	this work
(6)	rayon fiber textile	BmimOAc	115 °C	-	~ 56 %	~ 78	[20]
(12h)	filter paper	DMAc/LiCl	30 °C	-	< 20 %	~ 211	[41]
P 2-2	lyocell fabric	3% Cellulose in BmimCl	110 °C	1.00	-	~ 44	[44]
P 3-2	lyocell fabric	BmimCl	110 °C	1.32	-	~ 50	[44]
P60	VWR Grade 415 filter paper	EmimOAc	60 °C	1.31	~ 40 %	~ 123	[42]
linen	linen textile	BmimOAc	110 °C	-	~ 84 %	~ 47	[16]
rayon	rayon textile	BmimOAc	110 C		-	~ 70	[16]
Optimized sample	cotton textile + interleaf film	EmimOAc:DMSO=80:20	101 °C	1.42	-	~ 72	[43]
solvent/cell. 3-1	cotton textile	EmimOAc:DMSO=80:20	100 °C	0.91	~ 77 %	~ 57	[19]
solvent/cell. 3-1	cotton textile + interleaf film	EmimOAc:DMSO=80:20	100 °C	1.31	~ 66 %	~ 47	[19]
Flax-cell	flax nonwoven	BmimCl	80 °C	0.95	~ 66 %	~ 34	[21]
Lyocell-cell	lyocell nonwoven	BmimCl	80 °C	1.27	~ 63 %	~ 78	[21]
LC-0.5h	lyocell fabric	BmimCl	110 °C	0.97	~ 62 %	~ 30 (l) / ~ 36 (t)	[46]
LC-1h	lyocell fabric	BmimCl	110 °C	1.09	~ 57 %	~ 44 (l) / ~ 46 (t)	[46]
LC-2h	lyocell fabric	BmimCl	110 °C	1.32	~ 55 %	~ 43 (l) / ~ 48 (t)	[46]
LC-3h	lyocell fabric	BmimCl	110 °C	1.46	~ 53 %	~ 29 (l) / ~ 44 (t)	[46]
LC-4h	lyocell fabric	BmimCl	110 °C	1.47	~ 51 %	~ 28 (l) / ~ 42 (t)	[46]

* Abbreviations: BmimCl – 1-butyl-3-methyl imidazolium chloride; DMAc – dimethylacetamide; LiCl – lithium chloride; (l) – longitudinal; (t) - transversal

Selected References (Table ESI1.)

16. T. Huber, S. Pang, M.P. Staiger, All-cellulose composite laminates, *Composites: Part A* (2012), **43**: 1738-1745; <https://dx.doi.org/10.1016/j.compositesa.2012.04.017>
19. A. Victoria, M. E. Ries, P. J. Hine, Use of interleaved films to enhance the properties of all-cellulose composites, *Composites: Part A* (2022), **160**: 107062; <https://doi.org/10.1016/j.compositesa.2022.107062>

20. M. M. Salleh, K. Magniez, S. Pang, J. W. Dormanns, M. P. Steiger, Parametric optimization of the processing of all-cellulose composite laminae, *Manufact.: Polym. & Comp. Sci.* (2017), **3**: 73 – 79; <https://doi.org/10.1080/20550340.2017.1324351>
21. W. Gindl-Altmutter, J. Keckes, J. Plackner, F. Liebner, K. Eglund, M. P. Laboie, All-cellulose composites prepared from flax and lyocell fibres compared to epoxy–matrix composites, *Comp. Sci. Technol.* (2012), **72**: 1304 – 1309; <https://doi.org/10.1016/j.compscitech.2012.05.011>
41. T. Nishino, N. Arimoto, All-cellulose composite prepared by selective dissolving of fiber surface, *Biomacromolec.* (2007), **8**: 2712 – 2716; <https://doi.org/10.1021/bm0703416>
42. A. Victoria, P. J. Hine, K. Ward, M. E. Ries, design of experiments in the optimization of all-cellulose composites, *Cellulose*, (2023), **30**: 11013-11039; <https://doi.org/10.1007/s10570-023-05535-8>
43. B. Adak, S. Mukhopadhyay, A comparative study on lyocell-fabric based all-cellulose composite laminates produced by different processes”, *Cellulose* (2017), **24**: 835 – 849; <https://doi.org/10.1007/s10570-016-1149-x>
44. F. Chen, J. L. Bouvard, D. Sawada, C. Pradille, M. Hummel, H. Sixta, T. Budtova, Explore digital image correlation technique for the analysis of the tensile properties of all-cellulose composites, *Cellulose*, (2021), **28**: 4165-4178; <https://doi.org/10.1007/s10570-021-03807-9>
46. B. Adak, S. Mukhopadhyay, Effect of the dissolution time on the structure and properties of lyocell-based all-cellulose composite laminates, *J. App. Polym. Sci.*, (2016), 43398; <https://org.doi/10.1002/APP.43398>